

INFN/AE Torino
informi note

90/12

25 ottobre 1980

R. Bertoni, W. Fulgione, P. Galeotti, A. Giuliano,
N. Mengotti Silva, G.C. Trinchero
(INFN - Torino)

C. Ricci, S. Santini
(INFN - Firenze, Urbino)

LOW-ENERGY AND HIGH-ENERGY CALIBRATION OF THE
LVD LIQUID SCINTILLATION COUNTERS
IN THE GRAN SASSO LABORATORY

~~(april 1980)~~

INFN - LABORATORI NAZIONALI DEL GRAN SASSO

Introduction

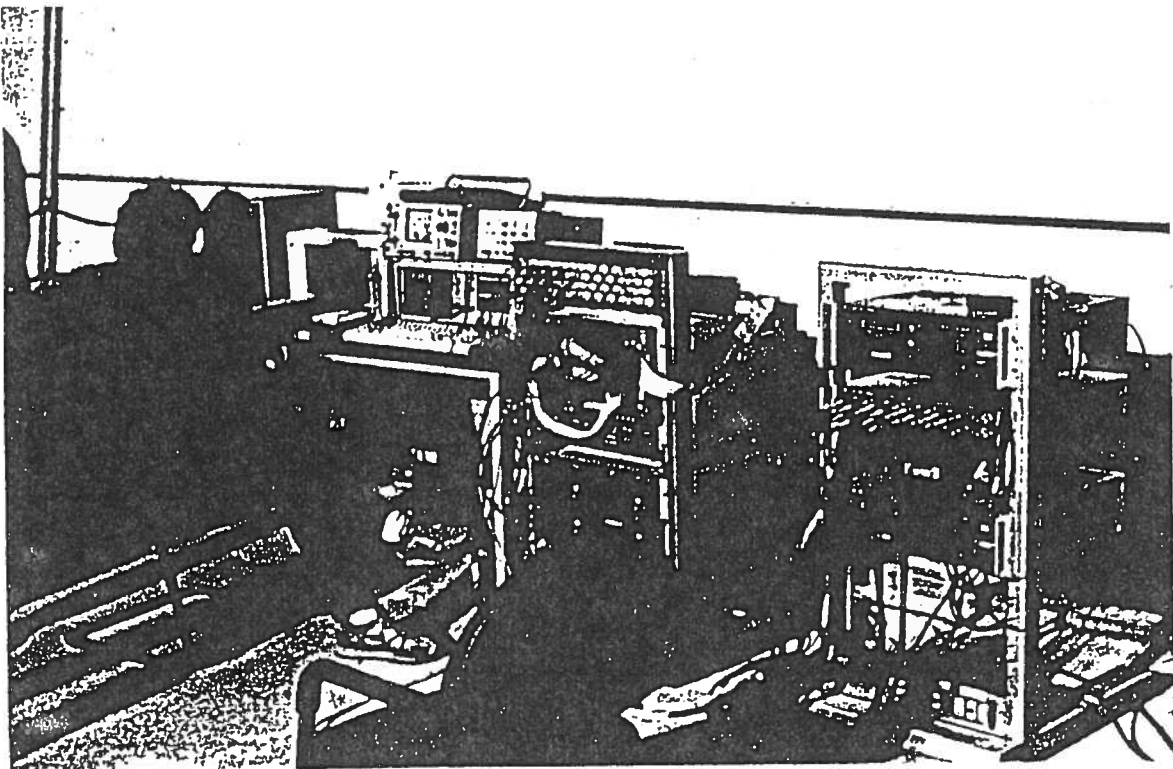
In this report we present the result of the measurements on the LVD liquid scintillator electronics performed in the underground laboratories of the Gran Sasso, during April '90.

6 scintillators counters, laying on the unshielded floor without iron containers, were forwarded to us by the LVD-INR group in the hall C of the LNGS. The hall C was chosen because of the non availability of the hall A where the real experiment is going to be mounted.

Our test concern the High Voltage power supply system and the electronics, based on the C1751B4 hybrid, connected with the photomultiplier signal of the liquid scintillator counters that will be used in the LVD neutrino experiment.

In §1 the experimental set up and the characteristics of the modules are described. The capability to recognize ν interactions from ν -e scattering (by the detection of (n, p, d, γ) capture signals) is discussed in § 2. The study of background conditions in this unshielded arrangement could be used as a comparison with future results, in the final configuration of the experiment.

The characteristics and energy calibration of the High Energy release channel are discussed in § 3.



§1 Electronics set up and Lab. tests

The electronic system, described in detail elsewhere [1], consists of:

- a trigger section performing a double discrimination for each PM signal (down to 100 μ Volts), and the trigger logic;
- a time to digital converter with a resolution of 12.5 nsec;
- a fast charge to digital converter, associated with the anodic pulses of the three PMs of each counter;
- an high range charge to digital converter to study very high energy release inside the liquid scintillator counter.

The block diagram of the electronics associated with one counter is shown in Fig.1, where one can see that the basic modules are the C-175, the charge and time digitizer C-176 [2] and the charge integrating ADC C-205 [3]. A complete test of the entire system was performed at the Istituto di Cosmogeofisica of Torino.

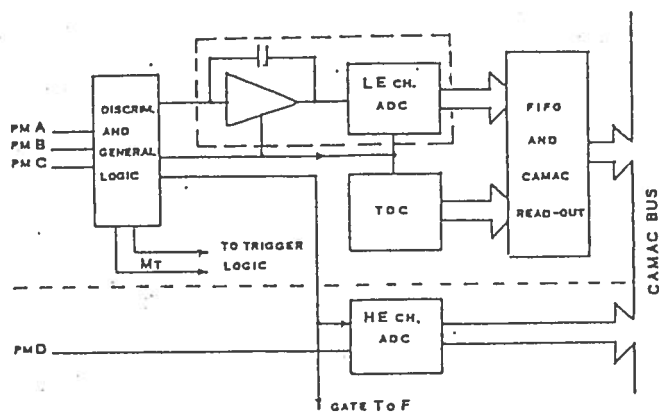


Fig.1 Electronics block diagram for a single counter.

The results of this test were stored on Vax Data Base and summarized on Tabs. 1 and 2. For each C-176 charge converter channel (Tab.1) there are reported: the pedestal with its r.m.s., the maximum σ value together with the linear coefficients of each segment and the integral nonlinearity.

For the C-205 32 channels (Tab.2), the two pedestals are reported with their r.m.s., the linear coefficients, the maximum σ values and the integral nonlinearity.

- [1] M.Aglietta, W.Fulgione, O.Saavedra, G.C.Trincherio
Nuclear Instruments and Methods, A277, (1989), 17-22
- [2] A.Bigongiari, W.Fulgione, D.Passuello, O.Saavedra, G.C.Trincherio
Nuclear Instruments and Methods, A05724 (1990), in print
- [3] F.Bourgeois, IEEE Trans. Nucl. Sc. NS-34, (1987), 240

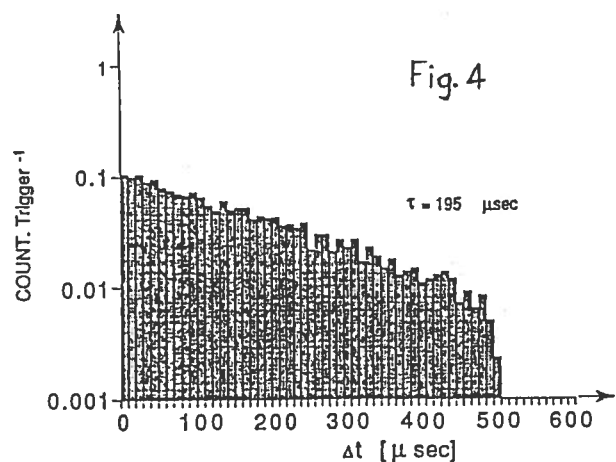
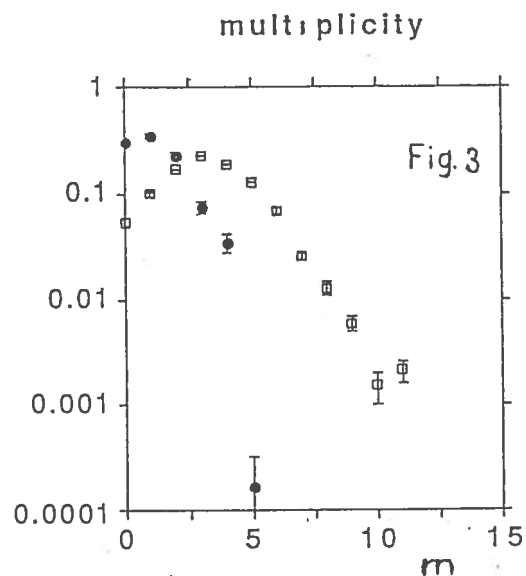
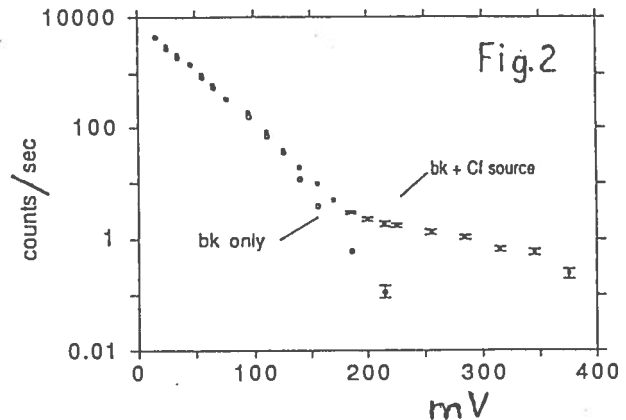
§2 (np,d γ) detection

Neutron detection with LVD is based on detecting the γ 's of 2.23 MeV energy emitted in the (np) capture reaction.

As a first step we measured: 1) the counting rate for different discrimination thresholds (see Fig.2). 2) the background spectrum 3) the time distribution of signals inside the 500 μ sec window after the trigger.

These background measurements are to be compared with the results obtained by putting a neutron source inside the detector. The used source is a ^{252}Cf which emits 3.7 neutrons per fission on the average. The trigger we used is given by the γ -prompt emitted during the fission.

The results of these measurements, for a threshold of 35 mV/PM, are shown in Fig.3,4 and 5. Fig.3 shows the multiplicity distribution of pulses, during a 500 μ sec gate, with and without the neutron source. The comparison between measured and expected average n number gives us an information on the n-detection efficiency. An independent information comes from the time distribution of these pulses after the fission signature. The expected mean life of thermalized neutron inside the scintillator is about 200 μ sec. Fig.4 shows the experimental time delay distribution obtained with a 35 mV threshold after subtracting the noise distribution at the same threshold level. The energy spectrum of the neutron candidates is shown in Fig.5.



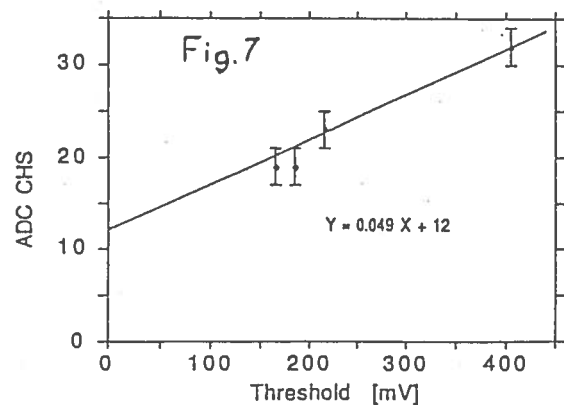
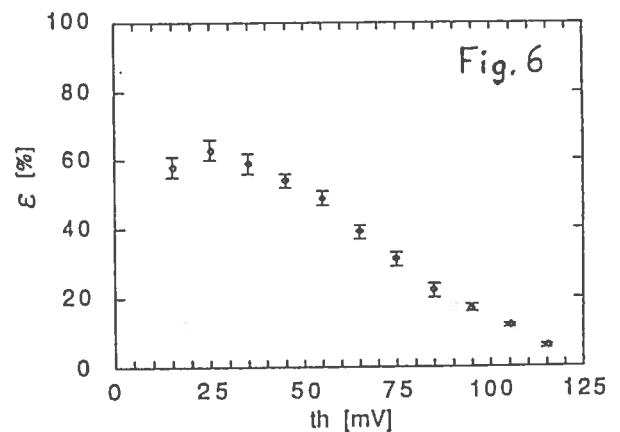
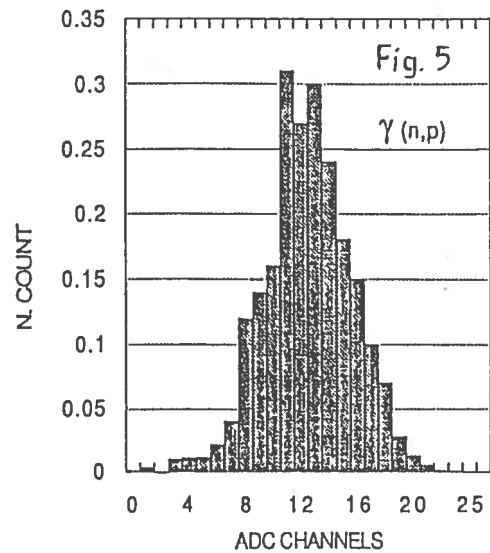
The chosen configuration based on the C1751B4 (see §3), while it is characterized by an high energy range, it does not permit a good energy resolution because the instrumental error becomes of the same order of the γ -capture energy release ($2\text{MeV}=0.5\text{pC}$).

The study of n-detection efficiency at different energy thresholds is shown in Fig.6. The plateau value of about 60% is in a good agreement with the results obtained with the Mont Blanc experiment. The working point can be chosen using this result together with the correspondent counting rate reported in Fig.2. The energy calibration of the C-176 charge converter is obtained by the muon spectrum (see Fig.8); one can use this result to calibrate the discriminator thresholds with the ADC spectra obtained for different thresholds: the result is shown in Fig.7.

§3 Muons and H.E.ch.

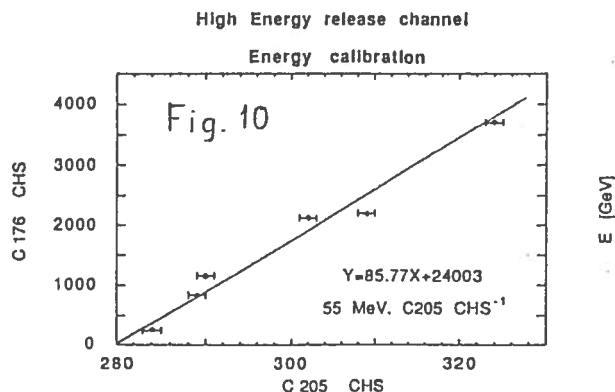
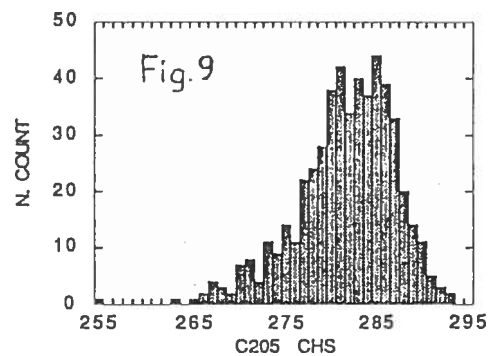
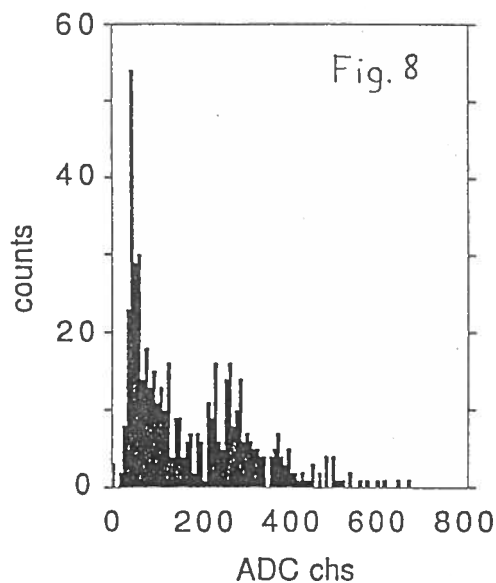
As can be seen from Fig.1, an independent channel associated with the 6th dinode PM signals is provided. This channel is used to study high energy release inside the detector, mostly due to muon interactions. The charge converter associated with this channel has a very high range, and time characteristics that match the expected frequency of this kind of events.

The charge integrating ADC C-205, described elsewhere [3], is a 32



channels double multiplexed charge to digital converter with a sensitivity of about 0.03 pC and a dynamical range of 15 bits. This devices can be calibrated in energy in two ways: a) by using the overlapping region with the C-176 converter or/and b) by the use of the single muon energy spectrum. Because no active device is present in the C-205 inputs, the only possibility that one has to increase the overlapping region is to moove the dynamics of the C-176 converter. Two different versions of the C-176 front end are provided, based on the two ibrids C 175IB4 and C 175IB4A. The diffrence consists on the mixer amplifier gain that can cange by a factor of 10.

We used, during this test, the C 175IB4 version with gain 1/3 on the sum. This means to have the maximum energy range for the so-called neutrino channel (up to about 3 GeV), and a wide overlapping region with the high-energy release channel. The muon energy spectrum for one counter, obtained with the two devices, is shown in figs. 8 and 9; even if the statistics is not rich, it is possible to identify the single particle spectrum from the background. Both with the C 175 and the C 205 the muon peak is clearly visible, and we wish to emphasize that in the second case it corresponds to only 0.1 pCoulomb. Fig.10 shows the functional relationship of the two modules in the entire overlapping region, with the first point given by the muon peak; the energy release to which the C 205 is sensitive reaches about 1 TeV/ch.



Conclusions

In spite of the electric noise actually present in the LNGS hall C, we have shown here the good capability of LVD to detect low and high energy pulses. In addition, since the detecting electronics was already tested in our home laboratory, it has also been checked that all these tests can be performed in a very short time.

The future final configuration of LVD, in hall A, with all the shielding mounted, will surely improve the signal to noise ratio. But already now the possibility, used in the Mont Blanc LSD experiment, to identify antineutrino interactions with a good signature (through the delayed gamma pulse from neutron capture after the main trigger signal) has been tested.

CH - 1	2.00000	647	17.24000	0.70686
	1.38187	0.07412	44.55632	0.55574
	0.74152	0.00475	54.37581	0.20152
	0.35781	0.00158	71.71733	0.30376
	0.17242	0.00051	146.01306	0.24111
	0.07058	0.00020	198.58977	0.20491
	0.03266	0.00019	248.25114	0.21907

CH - 2	1.50000	0	14.46000	0.80771
	1.39560	0.07412	41.62008	0.55574
	0.74032	0.00475	52.82831	0.27498
	0.36498	0.00161	90.61076	0.31076
	0.17521	0.00052	143.10322	0.24356
	0.09127	0.00022	196.69522	0.20212
	0.05447	0.00019	246.67032	0.22611

CH - 3	2.00000	661	15.45000	0.92060
	1.33242	0.07412	43.76236	0.55574
	0.73169	0.00467	54.07538	0.28363
	0.34972	0.00150	92.27400	0.29491
	0.16769	0.00050	145.49762	0.24095
	0.08810	0.00019	198.78186	0.19847
	0.05295	0.00020	247.48651	0.24520

CH - 4	1.50000	11	16.76000	0.66512
	1.38187	0.07412	43.44094	0.55574
	0.71226	0.00442	54.10370	0.27637
	0.34662	0.00148	91.70229	0.29610
	0.15774	0.00045	149.18211	0.22419
	0.08814	0.00020	197.60619	0.21095
	0.05281	0.00021	246.97626	0.25951

CH - 5	1.50000	0	13.37000	0.85621
	1.46134	0.06620	40.71229	0.53553
	0.75305	0.00484	52.82938	0.29758
	0.35763	0.00154	91.98656	0.29564
	0.16410	0.00047	148.65262	0.22789
	0.09913	0.00020	197.66147	0.20486
	0.05325	0.00020	246.98675	0.24695

CH - 6	1.00000	13	13.67000	0.95974
	1.32198	0.07412	42.26097	0.55574
	0.76678	0.00503	53.72829	0.27423
	0.36974	0.00163	91.87649	0.20512
	0.18440	0.00056	143.64812	0.25377
	0.09191	0.00020	198.43469	0.19680
	0.05489	0.00018	247.54388	0.20567

CH - 7	1.50000	7	18.71000	0.88651
	1.38182	0.09535	46.45000	0.60490
	0.76503	0.00484	54.79113	0.27970
	0.37522	0.00168	92.03748	0.31083
	0.18757	0.00058	143.10869	0.23760
	0.08975	0.00019	201.02962	0.18814
	0.05211	0.00018	251.12883	0.20857

CH - 8	1.00000	0	9.91000	0.86134
	1.45934	0.06620	40.14176	0.53553
	0.78709	0.00513	51.66041	0.20634
	0.37314	0.00166	91.41179	0.21051
	0.19204	0.00060	141.12531	0.26642
	0.09179	0.00020	199.21716	0.19457
	0.05488	0.00018	247.97397	0.20210

CH - 1	-2.51474	628
CH - 2	-2.37393	626
CH - 3	-3.20418	645
CH - 4	-4.84991	683
CH - 5	-3.45367	659
CH - 6	-1.98068	603
CH - 7	-2.91425	1617
CH - 8	-1.70639	592

Tab.1 - Calibration results of C-176
n.4

20	1	28.800	0.426	224.740	2.264	0.130	30.000	0.977	239.000	7.538	1.049	76	0.980	3.550	85	1.538
20	2	20.500	0.503	162.420	1.017	0.131	22.000	0.988	176.000	7.538	0.949	7	1.061	1.844	58	1.077
20	3	26.400	0.492	207.300	0.835	0.130	28.000	0.979	221.000	7.524	0.949	3	1.061	1.703	70	0.923
20	4	30.000	0.000	234.470	0.893	0.128	32.000	0.958	249.000	7.508	0.949	11	1.429	1.761	58	1.538
20	5	21.090	0.288	168.640	0.859	0.128	23.000	0.965	183.000	7.523	0.949	5	0.969	1.817	71	1.231
20	6	31.900	0.302	246.720	0.965	0.130	33.000	0.975	261.000	7.524	0.949	2	0.776	1.643	21	1.000
20	7	16.030	0.171	129.760	0.878	0.132	18.000	0.990	144.000	7.524	0.949	8	0.980	1.581	77	0.923
20	8	24.000	0.000	189.750	0.925	0.129	26.000	0.971	203.000	7.509	0.949	13	1.633	1.517	94	0.615
20	9	33.290	0.456	259.940	0.886	0.131	35.000	0.987	274.000	7.538	0.949	3	0.878	1.789	52	1.077
20	10	31.940	0.339	247.630	0.872	0.133	34.000	1.000	262.000	7.524	0.949	21	1.327	1.897	95	1.000
20	11	27.520	0.500	215.520	0.903	0.133	29.000	0.998	230.000	7.524	0.949	16	0.898	1.673	68	1.231
20	12	17.990	0.100	141.960	0.840	0.129	19.000	0.965	156.000	7.494	0.949	10	0.847	1.612	87	0.615
20	13	29.910	0.298	232.260	0.949	0.132	31.000	0.992	246.000	7.524	0.949	9	1.184	1.581	67	0.923
20	14	27.870	0.338	216.420	0.867	0.129	29.000	0.971	230.000	7.524	0.949	9	0.827	1.643	64	1.308
20	15	39.000	0.000	301.570	0.879	0.131	41.000	0.985	316.000	7.524	0.949	5	1.214	1.732	68	0.846
20	16	31.910	0.298	247.200	0.899	0.131	33.000	0.979	261.000	7.494	0.949	1	1.041	1.817	98	0.846
20	17	31.420	0.496	245.000	0.964	0.129	33.000	0.973	259.000	7.524	0.949	17	1.112	1.581	74	1.154
20	18	39.200	0.402	304.920	0.939	0.132	41.000	0.996	319.000	7.524	0.949	17	0.949	1.703	87	0.769
20	19	30.990	0.100	240.590	0.866	0.132	33.000	0.994	255.000	7.524	0.949	8	1.429	1.761	94	0.846
20	20	18.150	0.359	146.210	0.880	0.130	20.000	0.977	166.000	7.524	0.949	4	1.143	1.703	68	0.923
20	21	27.940	0.239	217.270	0.839	0.129	30.000	0.975	231.000	7.538	0.949	26	1.510	1.643	87	1.000
20	22	39.000	0.000	301.810	0.929	0.130	41.000	0.981	316.000	7.524	0.949	10	1.143	1.449	95	0.846
20	23	33.990	0.100	263.370	0.812	0.130	36.000	0.977	277.000	7.538	0.949	7	1.367	1.703	68	0.923
20	24	36.010	0.100	280.740	0.882	0.128	38.000	0.963	295.000	7.523	0.949	6	1.061	1.703	88	1.154
20	25	24.460	0.501	192.660	0.913	0.129	26.000	0.967	207.000	7.524	0.949	4	1.000	1.549	100	0.846
20	26	40.020	0.141	311.170	0.933	0.132	42.000	0.992	325.000	7.538	0.949	3	1.122	1.581	58	0.923
20	27	35.030	0.171	272.560	0.914	0.134	37.000	1.012	288.000	7.533	0.949	8	0.929	1.789	4	1.529
20	28	32.600	0.492	253.480	0.847	0.131	34.000	0.983	268.000	7.524	0.949	7	0.816	1.643	96	1.231
20	29	32.520	0.500	252.340	1.075	0.129	34.000	0.971	266.000	7.524	0.949	3	0.612	1.917	95	1.308
20	30	25.940	0.239	201.810	0.884	0.130	27.000	0.975	166.000	7.524	0.949	20	0.816	1.703	98	1.000
20	31	19.000	0.000	150.930	0.946	0.129	21.000	0.967	165.000	7.524	0.949	8	1.286	1.761	95	0.846
20	32	33.960	0.197	262.980	1.101	0.129	26.000	0.971	277.000	7.538	0.949	9	1.224	1.414	14	0.769

Tab.2 - Calibration results of C-205
n.20